Supporting Information

Construction of FeNi-Mo$_2$C@SiO$_2$ monolith electro catalyst with increased active sites and enhanced i ntrinsic activity toward water oxidation

Huanyu Chen, Jia-Qi Bai, Yuxue Wei, Jingshuai Chen,* Song Sun, and Chang-Jie Mao

Key Laboratory of Structure and Functional Regulation of Hybrid Materials (Ministry of Education), School of Chemistry and Chemical Engineering, Anhui University, Hefei, Anhui 230601, China.
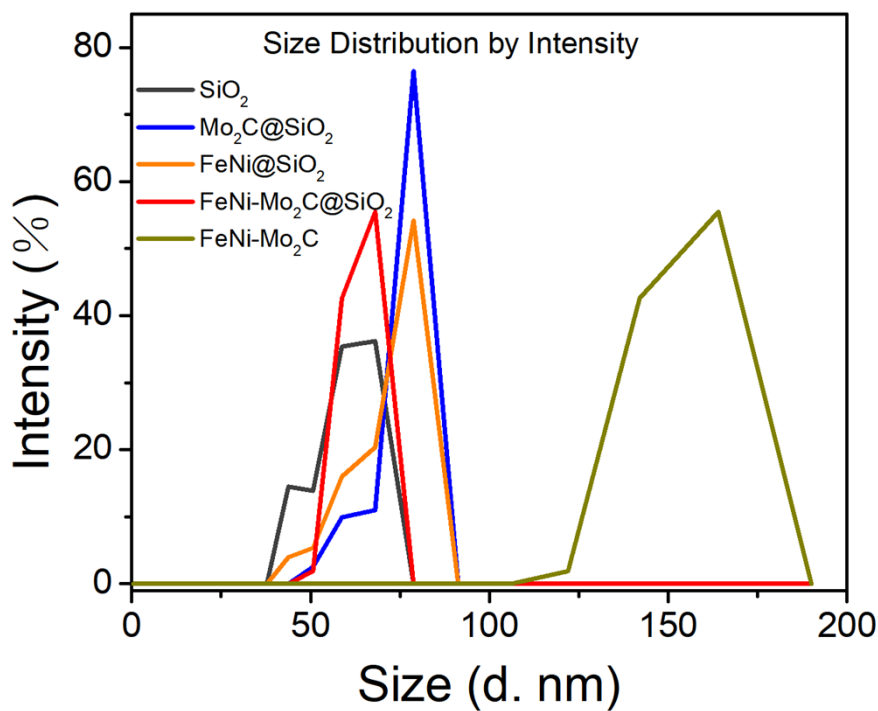
E-mail: chen_jshuai@ahu.edu.cn

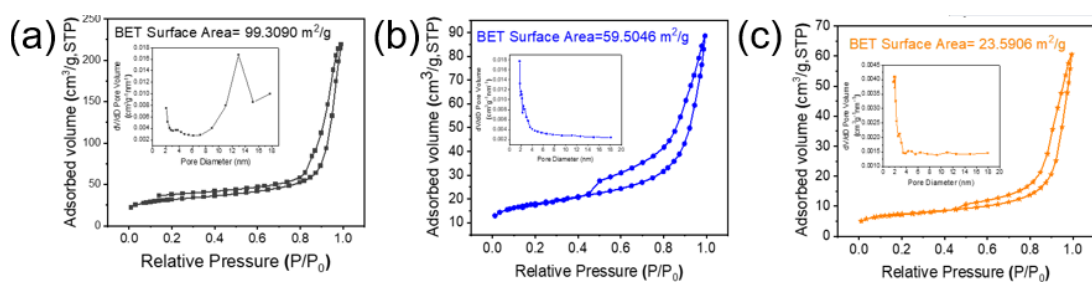Figure S1 Size distributions measured by Malvern laser particle size analyzer.

Figure S2 N$_2$ adsorption-desorption isotherms and pore size distribution (inset) of (a) SiO$_2$, (b)Mo$_2$C@SiO$_2$ and (c) FeNi-Mo$_2$C.
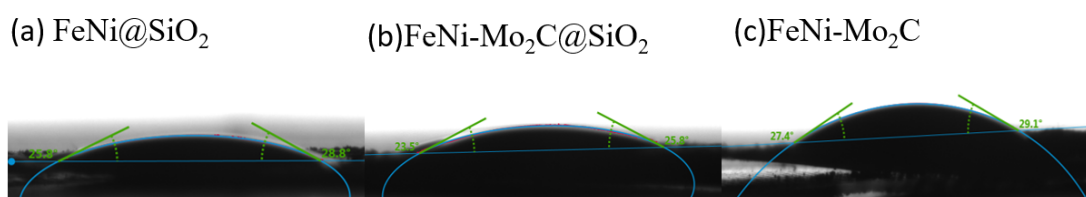
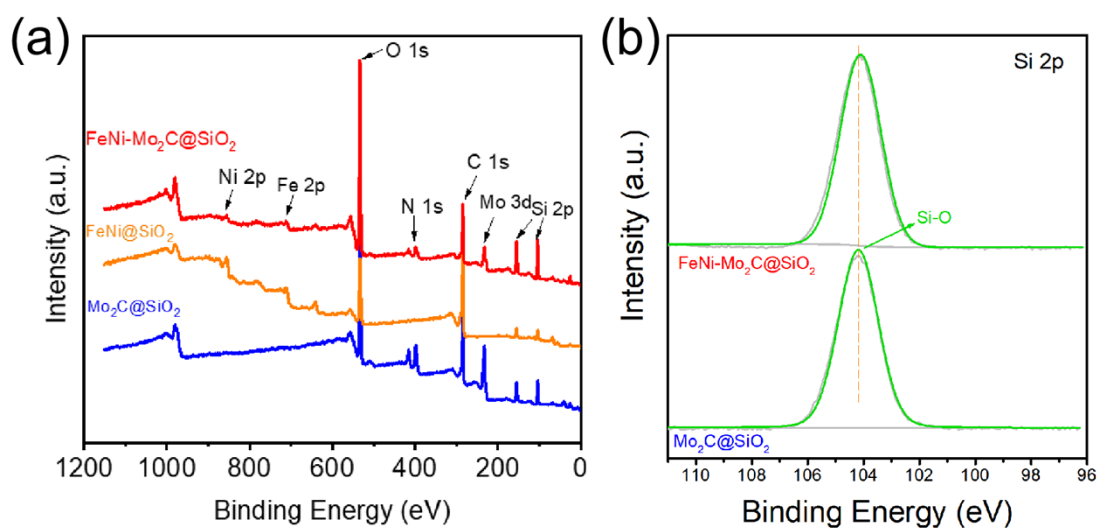Figure S3 Contact angles of (a) FeNi@SiO$_2$, (b) FeNi-Mo$_2$C@SiO$_2$, (c) FeNi-Mo$_2$C.

Figure S4 (a) XPS patterns of survey scan of FeNi-Mo$_2$C@SiO$_2$, FeNi@SiO$_2$ and Mo$_2$C@SiO$_2$. (b) High-resolution spectra of Si 2p of Mo$_2$C@SiO$_2$ and FeNi-Mo$_2$C@SiO$_2$.
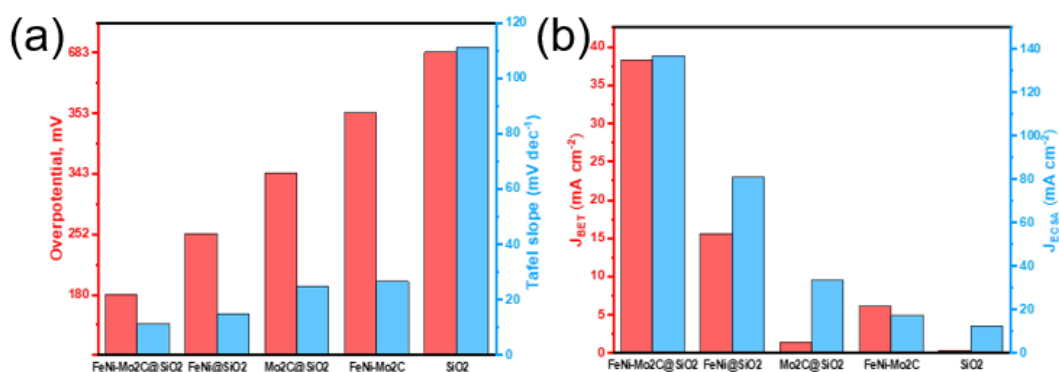

Figure S5 (a) Overpotential (red pillar) and Tafel slope (green pillar). (b) Comparison of BET surface area and ECSA normalized current density at 1.8 V (v
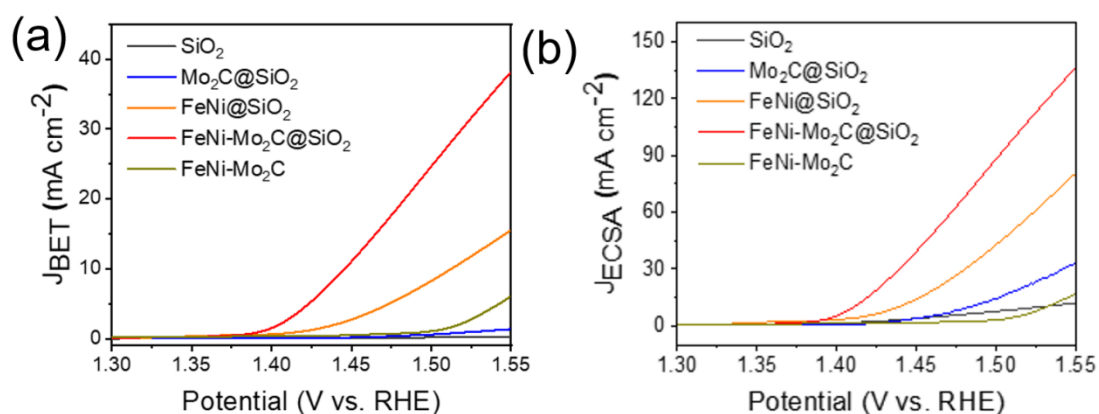
s. RHE).

Figure S6 (a) BET surface and (b) ECSA area normalized LSV curves for SiO_2, $FeNi@SiO_2$, $Mo_2C@SiO_2$, $FeNi-Mo_2C$ and $FeNi-Mo_2C@SiO_2$.

Table S1. OER activity comparison of $FeNi-Mo_2C@SiO_2$ catalyst with other FeNi-based, Ni-based or Mo-based electrocatalysts in 1.0 M KOH.

Catalyst	Overpotential (mV) at 10 mA cm^{-2}	Tafel slope (mV dec^{-1})	Reference
$FeNi-Mo_2C@SiO_2$	180	11.0	This work
Gd-NiFe-LDH@CC	210	40.9	J. Mater. Chem. A, 2021, 9, 2999-3006.
$NiFeO_xH_y$-C/CNTs/CFP	202	38.2	Chin. J. Catal., 2022, 9, 2354-2362.
60% $Fe_{0.5}Ni_{0.5}$/40% C	219	23.2	Small, 2022, 18, 2203340.
$FeNi(MoO_4)_x$@NF	227	47.5	Adv. Funct. Mater., 2022, 32, 2107342
Fe_1Ni_4-HHTP NWs	213	96	J. Mater. Chem. A, 2019, 7, 10431–10438.
$(Ni, Co)_{0.85}$Se	255	79	Adv. Mater., 2016, 28, 77.

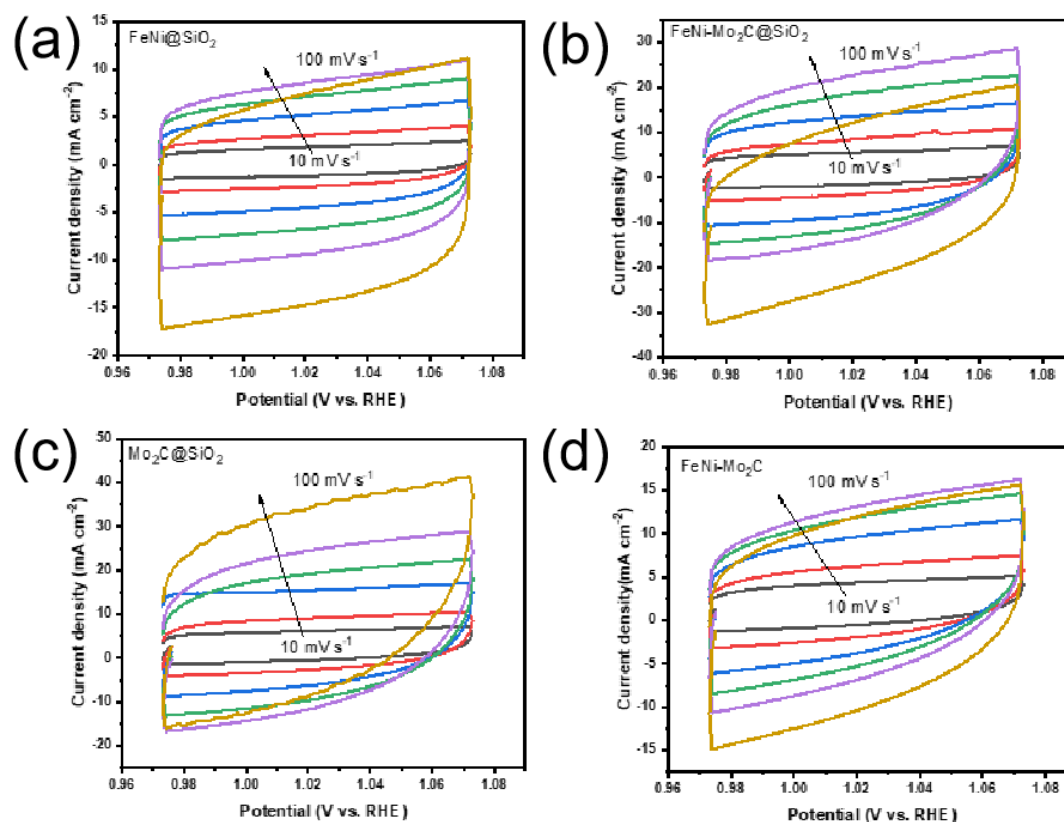|			
(Ni$_{0.77}$Fe$_{0.23}$) Se$_2$/CC	228	69	J. Mater. Chem. A, 2019, 7, 2831-2837.
NiCoSe$_2$/CC	255.8	71	J. Mater. Chem. A, 2018, 6, 17353-17360. Small, 2018, 14, 1800763.
NiSe-Ni$_{0.85}$Se/CP	300	98	Appl. Catal., B, 2019, 247, 107-114.
(Ni,Fe)S$_2$@MoS$_2$/CP	270	43.2	Mater. Today Energy, 2019, 11, 192–198.
Ni$_{0.8}$Fe$_{0.2}$-P/CC	278	41.2	J. Mater. Chem. A, 2018, 6, 3224-3230.
S-NiCoFe LDH	206	46	

Figure S7 CVs from 10 to 100 mV s^{-1} in a potential window between -0.05 V and 0.05 V (vs. Ag/AgCl) in 1 M KOH electrolyte: (a) FeNi@SiO$_2$, (b) Mo$_2$C @SiO$_2$, (c) FeNi-Mo$_2$C@SiO$_2$ and (d) FeNi-Mo$_2$C.
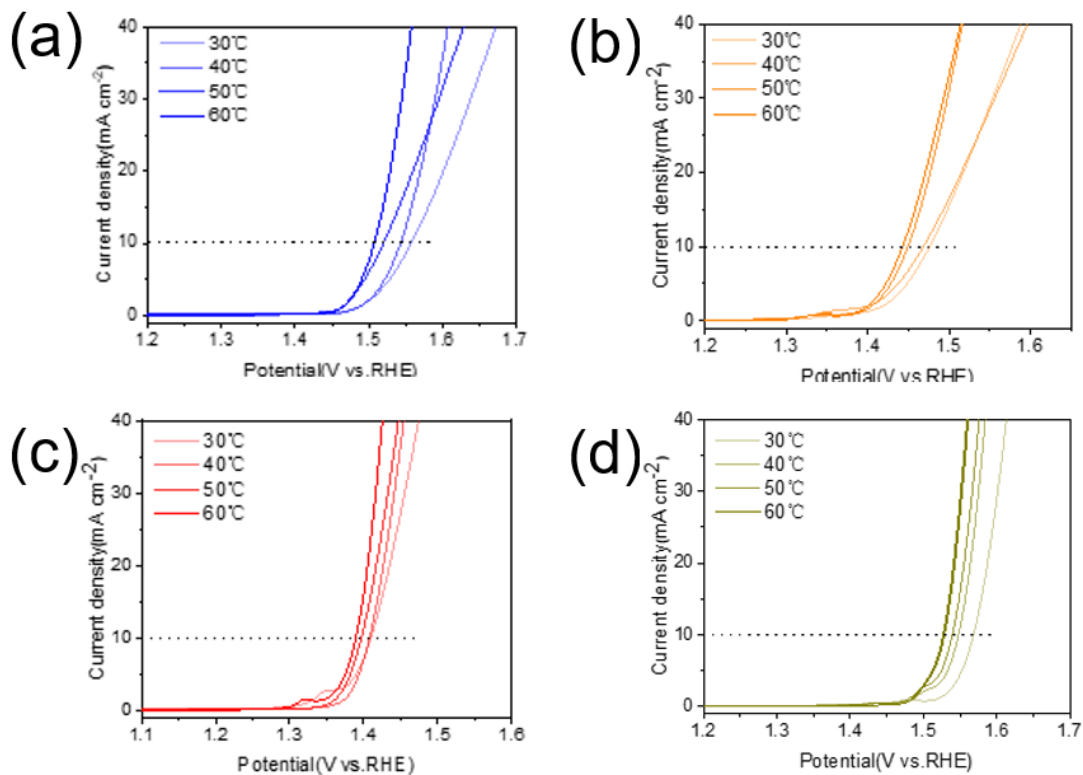
Figure S8 LSV curves recorded by increasing the electrolyte temperature for (a) $Mo_2C@SiO_2$, (b) $FeNi@SiO_2$, (c) $FeNi-Mo_2C@SiO_2$ and (d) $FeNi-Mo_2C$.
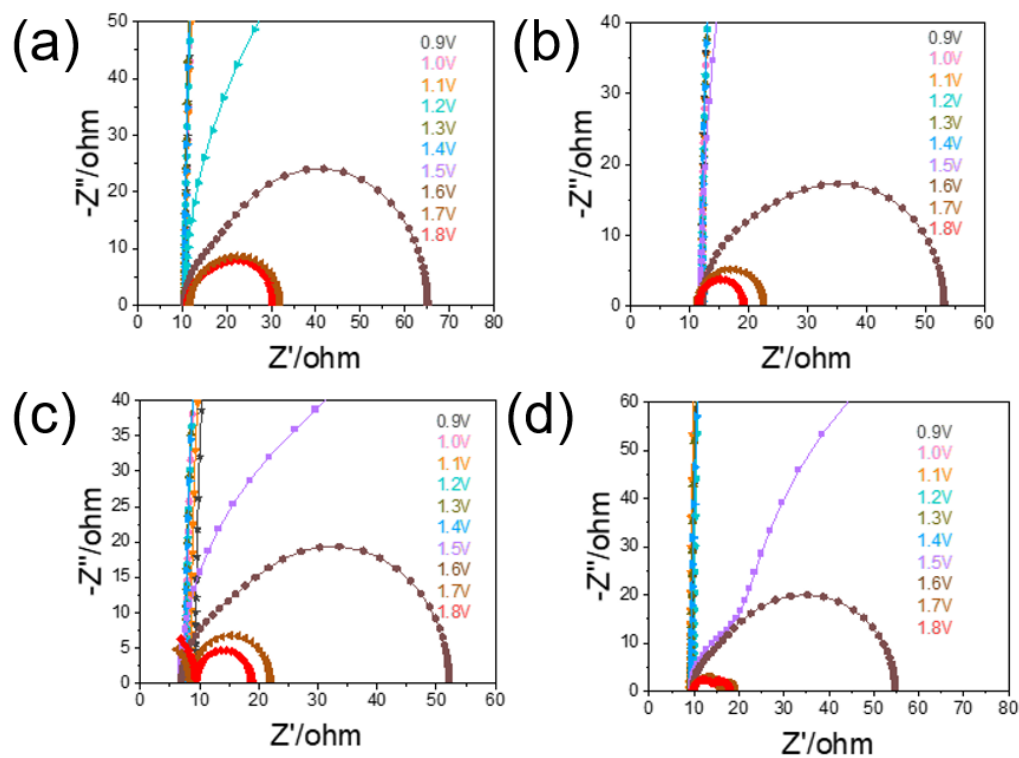
Figure S9 In-situ Electrochemical impedance recorded at potentials from 0.9 to 1.8 V (vs. RHE) for (a) $Mo_2C@SiO_2$, (b) $FeNi@SiO_2$, (c) $FeNi-Mo_2C@SiO_2$ and (d) $FeNi-Mo_2C$.

Figure S10 Equivalent circuit model. R_s represents a series resistance, R_{ct} refers to the total charge transfer resistance ($R_{ct} = R_1 + R_2$), C_{dl} and C_{ads} correspond to the double-layer capacitance and the intermediate adsorbed capacitance, respectively.

Table S2 Resistance and capacitance obtained by analysing the EIS spectra.

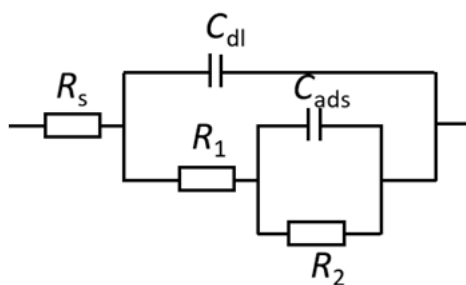| Samples	Potential (V vs.RHE)	R_s (Ω)	R_1 (Ω)	C_{dl} (μF)	R_2 (Ω)	C_{ads} (μF)	R_{ct} (Ω)
	0.9	34.86	10.73	11.75	1739	15.31	1749.73
	1.0	39.32	10.71	11.65	1826	15.73	1836.71
	1.1	30.89	10.66	12.28	1692	14.9	1702.66
	1.2	20.79	10.63	12.9	1989	17.85	1999.63
	1.3	14.5	10.65	13.23	2859	22.32	2869.65
Mo$_2$C@SiO$_2$	1.4	12.71	10.66	13.49	2524	23.15	2534.66
	1.5	5.06	10.68	14.42	157.9	22.89	168.58
	1.6	12.98	10.47	15.43	20.61	20.27	31.08
	1.7	7.726	11.29	14.47	11.52	20.49	22.81
	1.8	5.116	11.85	14.47	15.12	23.44	26.97
	0.9	21.43	12.11	14.29	1804	20.96	1816.11
	1.0	21.8	12.12	14.01	1797	19.29	1809.12
FeNi@SiO$_2$	1.1	21.41	12.13	14.79	1831	19.05	1843.13
	1.2	18.18	12.13	15.87	1787	21.17	1799.13
	1.3	15.23	12.13	17.14	1870	35.69	1882.13
	1.4	13.62	12.14	17.64	1915	39.46	1927.14
	1.5	5.135	12.03	22.49	637.4	34.35	629.43
	1.6	16.85	12.17	16.28	24.1	37	36.27
	1.7	1.207	11.43	15.72	10.06	45.98	21.49
	1.8	9.436	11.55	15.4	7.616	35.06	19.166
	0.9	13.87	38.53	18.63	1409	41.33	1447.53
	1.0	13.87	49.35	19.16	1563	40	1612.35

|						
FeNi-Mo$_2$C @SiO$_2$	1.1	13.36	37.76	19.45	1381	39.58	1418.76
	1.2	12.89	37.73	20.34	1423	41.28	1460.73
	1.3	11.29	37.62	20.9	1354	44.01	1391.62
	1.4	10.29	37.63	21.44	1312	45.2	1349.63
	1.5	2.232	36.79	30.08	79.31	75.43	116.1
	1.6	3.385	45.96	27.24	11.14	64.87	57.1
	1.7	1.673	21.49	49.03	12.02	56.09	33.51
	1.8	3.408	13.4	43.41	17.97	38.66	31.37
FeNi-Mo$_2$C	0.9	7.558	27.55	13.68	1748	15.98	1775.55
	1.0	8.199	27.73	14.72	1861	18.14	1888.73
	1.1	8.691	28.11	14.57	1668	20.36	1696.11
	1.2	8.433	27.95	14.03	1721	24.76	1748.95
	1.3	9.179	28.32	13.9	2875	31.07	2903.32
	1.4	9.925	29.38	13.76	2708	32.62	2737.38
	1.5	1.949	28.43	14.42	154.5	30.43	182.98
	1.6	4.258	9.656	15.24	5	21.11	26.886
	1.7	3.342	12.88	13.425	17.23	20.147	18.753
	1.8	3.427	12.79	13.46	5.873	20.373	17.479
					4.689		
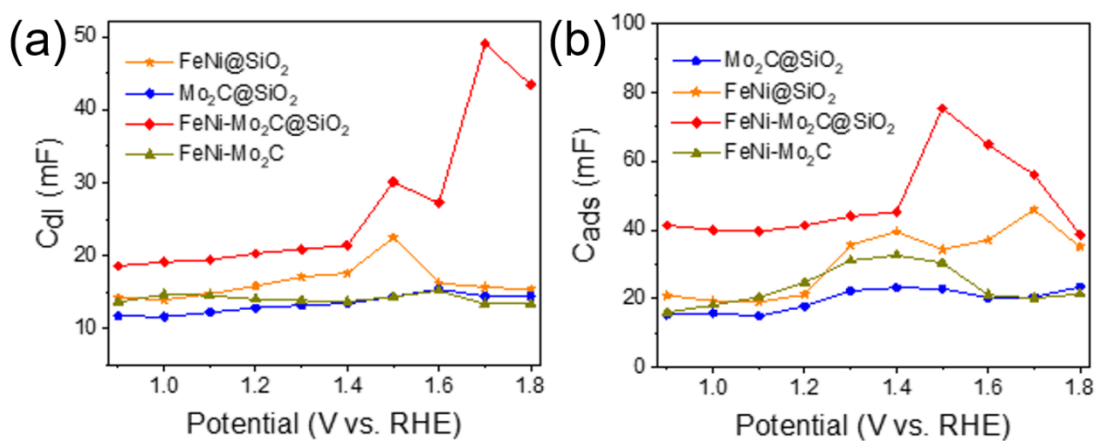
Figure S11 (a) C_{dl} and (b) C_{ads} with the increasing potential.